

## Coulomb Interactions and Mesoscopic Effects in Carbon Nanotubes

Charles Kane

*Department of Physics, University of Pennsylvania, Philadelphia, Pennsylvania 19104*

Leon Balents and Matthew P. A. Fisher

*Institute for Theoretical Physics, University of California, Santa Barbara, California 93106-4030*

(Received 7 August 1997)

We argue that long-range Coulomb forces convert an isolated  $(N, N)$  armchair carbon nanotube into a strongly renormalized *Luttinger liquid*. At high temperatures, we find anomalous temperature dependences for the interaction and impurity contributions to the resistivity, and similar power-law dependences for the local tunneling density of states. At low temperatures, the nanotube exhibits spin-charge separation, visible as an extra energy scale in the discrete tunneling density of states (for which we give an analytic form), signaling a departure from the orthodox theory of Coulomb blockade. [S0031-9007(97)04651-6]

PACS numbers: 71.10.Pm, 71.20.Tx, 72.80.Rj

The rapid experimental progress in controlled preparation of long, single-walled nanotubes bodes well both for applications and fundamental science [1]. Recent proposals for their use include tips for scanning microscopy, ultrastrong mechanical fibers, pinning sites for high- $T_c$  superconductors, and inclusions in composites for body armor. One of the most exciting prospects from the point of view of physics is that of a nearly ideal quantum wire. “Buckytubes” promise to be smaller, longer, cleaner, and more chemically manipulable than their semiconducting or metallic counterparts. For this purpose, probably isolated single-walled nanotubes are most relevant, and a thorough understanding of their electronic properties is desirable.

Previous papers by various authors have discussed the band structures in various geometries [2,3], as well as the effects of the electron-phonon [4] and short-range (Hubbard-like) electron-electron interactions [5,6]. These types of interactions have only weak effects, leading to a small linear correction to the resistivity at high temperatures [7], more significant deviations from noninteracting behavior occurring only at a very low temperature scale of order  $E_F e^{-N}$ , where  $E_F$  is the Fermi energy and  $N$  is the circumference of the tube in units of the graphene periodicity. While these treatments may be appropriate for arrays (“ropes”), they are inadequate for isolated nanotubes, due to the unscreened nature of the Coulomb interaction in this situation.

In this Letter, we address the effects of the long-range Coulomb potential on the most conducting “armchair” tubes. Once these are included, we find that significant deviations from noninteracting behavior should be observable *at all temperatures*. At high temperatures, an isolated armchair nanotube should behave as a Luttinger liquid, with an anomalous power-law dependence of the resistivity and power-law tunneling density of states, scaling differently at the end and center of the tube. At low

temperatures, Coulomb blockade behavior sets in, but with considerable deviations from the “orthodox theory” [8]. In particular, the conductance peak spacing is characterized by *three* energy scales in contrast to the usual two. In addition to the usual charging energy  $E_C$  and single-particle level spacing  $\epsilon_0$ , a third energy scale  $\epsilon_\rho$  reflects the separation of spin and charge in the 1D Luttinger liquid. Furthermore, a nontrivial ratio of peak heights is expected, arising from the collective nature of the low-energy excitations and invalidity of the quasiparticle picture. A full quantitative expression (for the tunneling density of states of a finite length nanotube) containing this physics, which holds away from half-filling and for sufficiently short tubes in the undoped case, is given in Eq. (10). A discussion of the experimental situation is given at the end of the Letter.

We begin by reviewing the band structure of the  $(N, N)$  armchair tube, which has been discussed by several authors. It is well captured by a simple tight-binding model of  $p_z$  electrons on the honeycomb lattice. For the armchair tubes, evaluating the resulting tight-binding band structure for the discrete set of allowed quantized transverse momenta  $q_y$  leads to only two gapless *one-dimensional* metallic bands (with  $q_y = 0$ ) [2,3]. These dominate the low-energy physics, disperse with the same velocity,  $v_F$ , and can be described by the simple 1D free Fermion model,

$$H_0 = \sum_{i,\alpha} \int dx v_F [\psi_{Ri\alpha}^\dagger i \partial_x \psi_{Ri\alpha} - \psi_{Li\alpha}^\dagger i \partial_x \psi_{Li\alpha}], \quad (1)$$

where  $i = 1, 2$  labels the two bands, and  $\alpha = \uparrow, \downarrow$  the electron spin.

We will make extensive use of the bosonized representation of Eq. (1), obtained by writing  $\psi_{R/L;i\alpha} \sim e^{i(\phi_{i\alpha} \pm \theta_{i\alpha})}$ , where the dual fields satisfy  $[\phi_{i\alpha}(x), \theta_{j\beta}(y)] = -i\pi \delta_{ij} \delta_{\alpha\beta} \Theta(x - y)$ . Expressed in these

variables (1) takes the form  $H_0 = \sum_{i,\alpha} \mathcal{H}_0(\theta_{i\alpha}, \phi_{i\alpha})$

$$\mathcal{H}_0(\theta, \phi) = \int dx \frac{v_F}{2\pi} [(\partial_x \theta)^2 + (\partial_x \phi)^2]. \quad (2)$$

The slowly varying electronic density in a given channel is given by  $\rho_{i\alpha} \equiv \psi_{Ri\alpha}^\dagger \psi_{Ri\alpha} + \psi_{Li\alpha}^\dagger \psi_{Li\alpha} = \partial_x \theta_{i\alpha} / \pi$ . The normal modes of  $\mathcal{H}_0$  describe long wavelength particle-hole excitations which propagate with a dispersion  $\omega = v_F q$ .

Turning to the interactions, a tremendous simplification occurs when  $N$  is large: the only couplings which survive in this limit are *forward scattering* processes which involve small momentum transfer. Roughly speaking, this can be understood as follows. “Interbranch” scattering processes (such as backscattering and umklapp) involve a momentum transfer of order  $2k_F \sim 1/a$ , where  $a$  is the carbon-carbon bond length. The matrix elements are therefore dominated by the *short-range* part of the interaction, at distances  $r \sim a$ , where the interaction changes significantly from site to site. However, the electrons in the lowest subband are spread out around the circumference of the tube, and for large  $N$  the probability of two electrons to be near each other is of order  $1/N$ . For the Coulomb interaction, the resulting dimensionless interaction vertices are of order  $(e^2/hv_F) \times 1/N$  [4,5]. By contrast forward scattering processes, in which electrons stay in the same branch, involve small momentum exchange. They are dominated by the *long-range* part of the Coulomb interaction, at distances larger than the radius, and there is no  $1/N$  suppression.

For  $N \geq 10$  it is thus appropriate to consider a *Luttinger model*, in which only forward scattering vertices are included. A further simplification arises because the *squared* moduli of the electron wave functions in the two bands are *identical* and spin independent. All the forward-scattering vertices can thus be written as a *single* interaction, coupling to the total charge density  $\rho_{\text{tot}} = \sum_{i\alpha} \partial_x \theta_{i\alpha} / \pi$ .

We will suppose that the Coulomb interaction is externally screened on a scale  $R_s$ , which is long compared to the tube radius  $R$ , but short compared to the length of the tube. For simplicity, we model this by a metallic cylinder of radius  $R_s$ , placed around the nanotube. From elementary electrostatics, the energy to charge the nanotube with an electron density  $e\rho_{\text{tot}}$  is

$$H_{\text{int}} = e^2 \ln(R_s/R) \int dx \rho_{\text{tot}}^2. \quad (3)$$

Since  $H_{\text{int}}$  involves only  $\rho_{\text{tot}}$  it is convenient to introduce a spin and channel decomposition via  $\theta_{i,\rho/\sigma} = (\theta_{i\uparrow} \pm \theta_{i\downarrow})/\sqrt{2}$  and  $\theta_{\mu\pm} = (\theta_{1\mu} \pm \theta_{2\mu})/\sqrt{2}$  with  $\mu = \rho, \sigma$ , and similar definitions for  $\phi$ . As defined, the new fields  $\theta_a$  and  $\phi_a$  with  $a = (\rho/\sigma, \pm)$  satisfy the same canonical commutators  $[\phi_a(x), \theta_b(y)] = -i\pi \delta_{ab} \Theta(x-y)$ . In the absence of interactions the Hamiltonian is simply  $H_0 = \sum_a \int_{x,\tau} \mathcal{H}_0(\theta_a, \phi_a)$ , which describes three “sectors” of neutral excitations and one charged excitation. Including the interactions only modifies the charge sector, which is described by the sum of two terms

$\mathcal{H}_\rho = \mathcal{H}_0(\theta_{\rho+}, \phi_{\rho+}) + H_{\text{int}}(\theta_{\rho+})$ , and may be written

$$\mathcal{H}_\rho = \int dx \frac{v_\rho}{2\pi} [g^{-1}(\partial_x \theta_{\rho+})^2 + g(\partial_x \phi_{\rho+})^2]. \quad (4)$$

This describes the 1D acoustic *plasmon* which propagates with velocity  $v_\rho = \sqrt{v_F[v_F + (8e^2/\pi\hbar) \ln(R_s/R)]}$  and is characterized by the Luttinger parameter  $g = v_F/v_\rho$ .

With repulsive forward-scattering interactions, the plasmon velocity  $v_\rho$  is larger than  $v_F$ , exhibiting the well known spin-charge separation of a 1D Luttinger liquid. Moreover, the Luttinger parameter,  $g$ , which equals one in a Fermi liquid is reduced. Since these effects are coming from long-ranged Coulomb forces and the short-ranged contributions are smaller—down by  $1/N$ —it is possible to make *semiquantitative* estimates of Luttinger liquid effects. Specifically, with a Fermi velocity estimated from graphite band structure of  $v_F = 8 \times 10^5$  m/s and a screening length of, say, 1000 Å, one finds  $g \approx 0.2$ —well below the Fermi liquid value,  $g = 1$ . This result is relatively insensitive to the screening, depending only logarithmically on the length  $R_s$ .

Physical properties can be readily evaluated from Eqs. (2) and (4). For example, consider the density of states to tunnel an electron into a long nanotube from a metallic electrode or perhaps a scanning tunneling microscopy (STM) tip. Upon expressing the electron operator in terms of the boson fields and evaluating the electron Green’s function one finds  $\rho_{\text{tun}}(\epsilon) \sim \epsilon^\alpha$ , with an exponent  $\alpha = (g + g^{-1} - 2)/8$ , which vanishes in the Fermi liquid limit ( $g = 1$ ), but is expected to be quite appreciable,  $\alpha \approx 0.4$  for the nanotube. The resulting tunneling current should be suppressed with  $dI/dV \sim V^\alpha$ , and the linear conductance  $G(T) \sim T^\alpha$  vanishing with temperature. This suppression is even more dramatic for tunneling into the *end* of a long nanotube. One finds a larger exponent,  $\alpha_{\text{end}} = (g^{-1} - 1)/4 \approx 1$ .

These results were established under the assumption that the backward and umklapp interactions could be safely ignored. Since their bare values are small, of order  $1/N$ , this might seem very reasonable. However, the presence of the strong forward scattering greatly modifies the effects of the umklapp scattering at low energies, so caution is necessary. To estimate this effect we reconsider the neglected interactions as perturbations upon the Luttinger model. We find that the momentum-conserving backward-scattering vertices,  $u_{bs}$ , are “marginal.” They only become important at an exponentially small energy scale,  $\Delta_{bs} \sim E_F \exp(-c/u_{bs})$  with an order one constant,  $c$ . At half-filling, however, the umklapp scattering vertices  $u$  grow much more rapidly at low energies due to the stiff plasmon mode. Their renormalized strengths at energy  $\epsilon$  grow as  $u(\epsilon) \sim u(E_F/\epsilon)^{1-g}$ . This growth signifies the development of a gap in the spectrum, with magnitude  $\Delta \sim E_F u^{1/(1-g)}$ . The above Luttinger liquid results are valid only on energy scales well above this gap, where the umklapp scattering can still be safely ignored. Unfortunately, a reliable quantitative estimate for this gap

is difficult. For nanotubes doped away from 1/2 filling, umklapp processes suffer a momentum mismatch at the Fermi surface, thereby becoming ineffective. In particular, for a doped tube with Fermi energy shifted away from the band center by an energy  $\delta$  which satisfies  $u(\delta) \ll 1$  ( $\delta \gg E_F/N^{1/(1-g)}$  for  $e^2/\hbar v_F$  of order one), the validity of the Luttinger model should be limited only by the exponentially low backscattering scale  $\Delta_{bs}$ .

In an undoped tube, at temperatures above the energy gap, one expects the umklapp interactions to cause weak backscattering and lead to a nonzero resistivity [9]. The resistivity should be proportional to the electron backscattering rate, varying as  $\rho(T) \sim u(T)^2 T$ , where  $u(T) \sim T^{g-1}$  is the energy (temperature) dependent umklapp scattering strength. The resulting nonlinear power-law behavior,  $\rho(T) \sim T^{2g-1}$ , valid over a temperature range above the gap, is a clear signature of the Luttinger liquid. For temperatures below the gap, this should cross over into an activated form, diverging exponentially as  $T \rightarrow 0$ . Backscattering mediated by twiston phonons (if unpinned by the substrate) should lead to the same temperature dependence. Impurities also have dramatically enhanced effects in the Luttinger liquid [10]. Like umklapp and twiston scattering, disorder leads to a high-temperature power-law resistivity, but with  $\rho(T) \sim T^{-(1-g)/2}$ .

The above discussion has implicitly assumed that the nanotube is *infinitely* long. For a tube with finite length,  $L$ , many interesting mesoscopic effects are expected. For temperatures and/or voltages well above the level spacing  $\pi\hbar v_F/L$ , the above results (for  $L = \infty$ ) should be valid. We now turn to a discussion of the mesoscopic effects on smaller energy scales. For simplicity, we assume that  $L$  is sufficiently small so that the energy gaps induced by umklapp and backward scattering satisfy  $\Delta, \Delta_{bs} \ll \hbar v_F/L$ . In this limit, it is valid to employ the Luttinger model.

For a finite tube it is convenient to express  $\theta_a, \phi_a$  in terms of creation and annihilation operators for the discrete bosonic excitations. At the tube ends, these fields must satisfy the boundary conditions  $\partial_x \phi(x=0, L) = 0$  and  $\theta_a(L) - \theta_a(0) = (\pi N_a + \delta_a)/2$ , where  $N_a$  is the integer charge in the  $a$  sector and  $\delta_a$  is a sum of phase shifts associated with the tube ends [11]. Expanding in a Fourier series gives

$$\theta_a(x) = \sum_{m=1}^{\infty} \sqrt{\frac{g_a}{m}} i \sin\left(\frac{m\pi x}{L}\right) (b_{am} - b_{am}^\dagger) + \theta_a^{(0)}(x), \quad (5)$$

$$\phi_a(x) = \sum_{m=1}^{\infty} \sqrt{\frac{1}{g_a m}} \cos\left(\frac{m\pi x}{L}\right) (b_{am} + b_{am}^\dagger) + 2\Phi_a, \quad (6)$$

where the zero-mode term  $\theta_a^{(0)} \equiv \frac{x}{2L}(\pi N_a + \delta_a)$ . The  $b_{am}$  satisfy  $[b_{am}, b_{a'm'}^\dagger] = \delta_{aa'} \delta_{mm'}$  and the operators  $N_a$  and  $\Phi_a$  satisfy  $[N_a, \Phi_{a'}] = i\delta_{aa'}$ . Here we adopt the notation  $g_{\rho+} = g$  and  $g_a = 1$  for the three neutral sectors. Substituting (5) and (6) into (2) and (4), we may express the Hamiltonian as  $\mathcal{H} = \sum_a \mathcal{H}_a - \mu N_{\rho+} -$

$\Delta_B N_{\sigma+} + \varepsilon_{\text{cap}} N_{\rho-}$ , where we have included a chemical potential  $\mu$  controlled by external gates, a Zeeman splitting  $\Delta_B$ , and  $\varepsilon_{\text{cap}} = \pi v_F \delta_{\rho-}/4L$  [11]. Moreover,

$$\mathcal{H}_a = \frac{\varepsilon_a}{8g_a} N_a^2 + \sum_{m=1}^{\infty} m \varepsilon_a b_{am}^\dagger b_{am}, \quad (7)$$

where  $\varepsilon_\rho = \pi\hbar v_\rho/L$  and  $\varepsilon_a = \varepsilon_0 = \pi\hbar v_F/L$  for the neutral sectors.

Consider the local tunneling density of states,  $A(x, \varepsilon) = \sum_s |\langle s | \psi^\dagger(x) | 0 \rangle|^2 \delta(E_s - E_0 - \varepsilon)$ , which is proportional to  $dI/dV$  measured in a tunneling experiment. This probes many body states  $s$  in which one electron has been added to the system at  $x$ . The zero mode changes  $N_a$  by  $\pm 1$  depending on the spin and band of the added electron. In addition, any number of collective modes may be excited. Because of the structure of the bosonic excitation spectrum and the fact that three of the four  $\varepsilon_a$ 's are equal, many of these excited states will be degenerate.  $A(\varepsilon)$  thus consists of a series of peaks,

$$A(\varepsilon) = \sum_{n_\rho n_0} C_{n_\rho n_0} \delta[E_C + \varepsilon_0(n_0 + \frac{1}{2}) + \varepsilon_\rho n_\rho - \varepsilon], \quad (8)$$

where  $n_0$  and  $n_\rho$  are non-negative integers and the Coulomb energy is given by  $E_C = (e^2/L) \ln R_s/R = \sum_a \pi\hbar v_a/8Lg_a - \varepsilon_0/2$ . For simplicity we have set  $\mu = \Delta_B = \varepsilon_{\text{cap}} = 0$ . Since these terms couple only to the zero modes  $N_a$ , their effect is to introduce a constant shift in energy of all of the peaks for a given  $N_a$ . Each of the peaks will thus in general be split into four by  $\Delta_B$  and  $\varepsilon_{\text{cap}}$ , and varying  $\mu$  causes a constant shift in the energies of all the peaks.

The amplitudes of the peaks in  $A(x, \varepsilon)$  may be determined by computing the local Green's function  $G(x, t) = \langle \psi(x, 0) \psi^\dagger(x, t) \rangle = \int_0^\infty d\varepsilon A(x, \varepsilon) e^{i\varepsilon t}$ . Expressing  $\psi(x)$  in terms of the boson operators, this takes the form  $G(t) = \prod_a \mathcal{G}_a(t)$ , where  $\mathcal{G}_a(t) = \langle O_a(t) O_a^\dagger(0) \rangle$ , with  $O_a = \exp[i(\phi_a \pm \theta_a)/2]$ . We then find

$$\mathcal{G}_a = \left[ \frac{(\pi/L) e^{i\varepsilon_a t/2}}{1 - e^{i\varepsilon_a t}} \right]^{2g_a^\pm} \left[ \frac{4 \sin^2(\pi x/L) e^{i\varepsilon_a t}}{(1 - z e^{i\varepsilon_a t})(1 - z^* e^{i\varepsilon_a t})} \right]^{g_a^\mp}, \quad (9)$$

where  $g_a^\pm = (g_a^{-1} \pm g_a)/16$  and  $z = \exp 2\pi i x/L$ . By formally expanding  $G(x, t)$  in powers of  $e^{i\varepsilon_a t}$  it is then straightforward to extract the ratios

$$C_{n_\rho n_0}/C_{00} = c_{3/4}^{n_0} \sum_{0 \leq i \leq j \leq n_\rho} c_{2g^+}^{n_\rho-j} c_{g^-}^{j-i} c_{g^-}^i z^{j-2i}, \quad (10)$$

where  $c_g^n = \Gamma(g+n)/\Gamma(g)\Gamma(1+n)$ .

In Fig. 1 we plot the resulting density of states for tunneling into the end and the middle of a tube for  $\mu = B = \varepsilon_{\text{cap}} = 0$ . The tunneling spectrum is characterized by three energy scales. As in the orthodox theory of the Coulomb blockade,  $E_C$  sets the minimum energy for adding an electron to the tube. The excited states

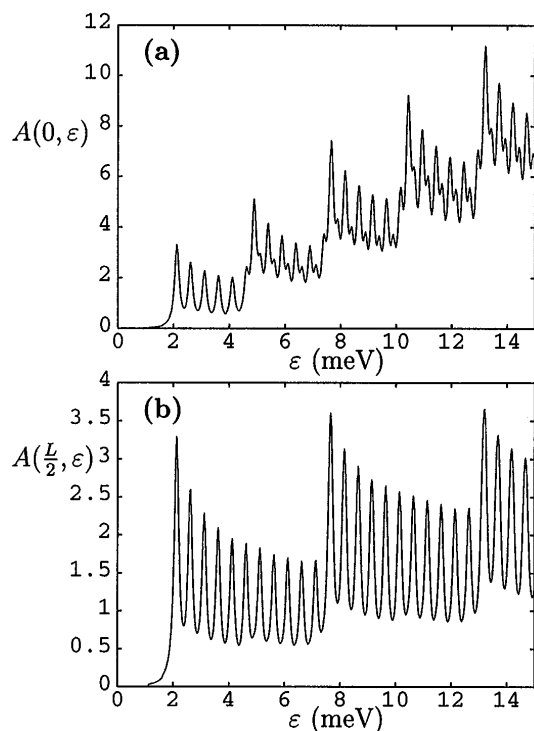


FIG. 1. Local tunneling density of states (a) at the end and (b) in the center of the nanotube, shown for a nanotube of length  $L = 3 \mu\text{m}$  and  $g = 0.18$ . We have phenomenologically introduced a rounding to the spectral peaks, as would appear due to the Fermi distribution in the leads in a tunneling experiment.

fall into two categories: The quantized spin/ﬂavor excitations have energy  $\varepsilon_0 = \pi \hbar v_F / L$ —the unrenormalized level spacing of the single electron states. These correspond to *neutral* collective excitations which are unaffected by the long-range Coulomb interaction. In addition, however, there are charged “quantized plasmon” excitations, which have an energy  $\varepsilon_\rho = \varepsilon_0 / g = \sqrt{\varepsilon_0(8E_C + \varepsilon_0)}$ . This third energy scale is a signature of charge-spin separation—the hallmark of a Luttinger liquid. Since  $\varepsilon_\rho > \varepsilon_0$ , the peaks in Fig. 1 fall into distinct families with different plasmon excitations. In particular, the lowest family corresponds to tunneling into the ground state of the charge sector. The next family corresponds to exciting a single quantum of the lowest energy plasmon: a dipole resonance.

The ratios of the peak heights contain detailed information about the interactions. Within a given family,  $C_{n_p, n_0} / C_{n_p, 0} = c_{3/4}^{n_0}$ , which is  $3/4$  for  $n_0 = 1$  and approaches  $n_0^{-1/4} / \Gamma(3/4)$  for  $n_0 \geq 3$ . The amplitude ratios between families depends on the tunneling location  $x$ . For the first plasmon excitation,  $C_{10} / C_{00} = 2[g_+ + g_- \cos(2\pi x / L)]$ . Thus, as shown in Fig. 1(b), the amplitude of the dipole resonance is suppressed when tunneling into the middle of the tube.

It should be interesting in the future to explore both the low- and high-temperature regimes experimentally. We expect that in a fairly clean experimental system, the

power-law resistivity  $\rho(T) \sim u^2 T^{2g-1} + n_0 T^{-(1-g)/2}$  is perhaps the most easily testable prediction. A potentially more rewarding experiment would be to measure the tunnel conductance of an isolated nanotube with an STM, as a function of bias, external gate potential, and position along the tube, which we expect to be directly proportional to  $A(x, \varepsilon)$ . Clustering into families, as shown in Fig. 1, would give direct and dramatic experimental evidence for the elusive charge-spin separation of a Luttinger liquid. In addition to Coulomb blockade behavior, the current-voltage curves observed by Tans *et al.* [8] display interesting structure, with signatures of a discrete energy level spacing  $\varepsilon_0 \approx 0.4$  meV and an additional 2 meV step which may be related to the lowest plasmon excitation. However, a detailed comparison with the simple Luttinger model may be complicated, since the predicted form requires (1) negligible impurities; (2) sufficiently short tubes and/or doping such that  $\Delta, \Delta_{bs} \ll \varepsilon_0$ ; and (3) large-scale uniformity of the gate potential and other external perturbations. Nonetheless, a systematic study of the tunneling characteristics would be most useful at both low and high voltages and temperatures. We encourage mesoscopic experimentalists to rise to the challenge of tunneling measurements in the Luttinger regime.

It is a pleasure to thank A. T. Johnson and E. J. Mele for helpful discussions, and especially C. Dekker and S. Tans for sharing experimental results. This work has been supported by the National Science Foundation under Grants No. PHY94-07194, No. DMR94-00142, No. DMR95-28578, and No. DMR95-05425.

- 
- [1] T. W. Ebbesen, *Phys. Today* **49**, No. 6, 26 (1996).
  - [2] N. Hamada *et al.*, *Phys. Rev. Lett.* **68**, 1579 (1992); J. W. Mintmire *et al.*, *Phys. Rev. Lett.* **68**, 631 (1992); R. Saito *et al.*, *Appl. Phys. Lett.* **60**, 2204 (1992).
  - [3] X. Blase, L. X. Benedict, E. L. Shirley, and S. G. Louie, *Phys. Rev. Lett.* **72**, 1878 (1994); C. L. Kane and E. J. Mele, *Phys. Rev. Lett.* **78**, 1932 (1997).
  - [4] C. L. Kane *et al.*, *cond-mat/9704117*.
  - [5] L. Balents and M. P. A. Fisher, *Phys. Rev. B* **55**, 11973 (1997).
  - [6] Y. A. Krotov, D. H. Lee, and S. G. Louie, *Phys. Rev. Lett.* **78**, 4245 (1997).
  - [7] Such behavior has been observed in ropes. See A. Thess *et al.*, *Science* **273**, 483 (1996); J. E. Fischer *et al.*, *Phys. Rev. B* **55**, R4921 (1997).
  - [8] Coulomb blockade behavior has been observed in single nanotubes by S. J. Tans *et al.*, *Nature (London)* **386**, 474 (1997). It has also been seen in ropes by M. Bockrath *et al.*, *Science* **275**, 1922 (1997).
  - [9] T. Giamarchi and A. J. Millis, *Phys. Rev. B* **46**, 9325 (1992).
  - [10] T. Giamarchi and H. Schulz, *Phys. Rev. B* **37**, 325 (1988).
  - [11] These phase shifts depend upon the microscopic structure of the cap, but are expected to be spin independent.